

Copyright 2012 IEEE.

Published at the **2012 IEEE 19th International Conference on Image Processing (ICIP 2012)**, scheduled for September 30 to October 3, 2012 in Lake Buena Vista, Orlando, FL, USA.

Personal use of this material is permitted. Permission from IEEE must be obtained for all other uses, in any current or future media, including reprinting/republishing this material for advertising or promotional purposes, creating new collective works, for resale or redistribution to servers or lists, or reuse of any copyrighted component of this work in other works.

THE IMPORTANCE OF THE NORMALIZING CHANNEL IN LOG-CHROMATICITY SPACE

Eva Eibenberger^{1,2}, Elli Angelopoulou^{1,2}

¹Pattern Recognition Lab, University of Erlangen-Nuremberg, Germany

²Erlangen Graduate School in Advanced Optical Technologies (SAOT), Erlangen, Germany
 {eva.eibenberger, elli.angelopoulou}@informatik.uni-erlangen.de

ABSTRACT

The log-chromaticity space (LCS) is a color space with excellent illumination-invariant properties. When converting RGB colors to LCS, there exist four different options for choosing the normalizing channel. For classification applications, we analyze the impact of the normalizer on the distribution of colors in LCS. Based on synthetic and real image data we show that the geometric mean does not introduce a bias to the color clusters and always results in an intermediate clustering performance. However, data-specific selection of the normalizing channel can further improve the results. For instance, for skin classification we show that using the blue channel as denominator results in a recognition improvement of about 25.9% compared to the red channel (worst result). In comparison to the geometric mean and the green channel, the two most popular denominators, the performance increase is 12.9% and 2.9%.

Index Terms— Color, log-chromaticity space, classification

1. INTRODUCTION

Color information is a popular cue in many computer vision applications, like object detection, recognition, image retrieval or tracking. Compared to shape information, color cues are relatively robust to changes in scale and orientation. However, using color information on arbitrary images can be challenging. The appearance of an object's color is affected by different factors, such as illumination, scene geometry, camera characteristics and scene materials. The use of an appropriate color space can greatly facilitate the effective employment of color data.

A color space providing excellent properties for illumination adaptation is the *log-chromaticity space (LCS)* [1]. The transformation of image intensities $(i_r, i_g, i_b)^T$ to LCS is obtained by computing color ratios (e.g. $\frac{i_r}{i_g}, \frac{i_b}{i_g}$) and then applying the natural logarithm to these ratios. Under the assumption of Lambertian reflectance and narrow bands, the LCS has two important properties: (a) the LCS colors of a certain uniform-albedo surface seen under different illumination colors tend to lie on a straight line in LCS (b) these lines of different surfaces are parallel to each other.

When converting to LCS, one can choose to use one of the following four normalizing channels for the color ratios: either one of the RGB channels itself, i.e. i_c where $c \in \{r, g, b\}$, or their geometric mean, i.e. $(i_r i_g i_b)^{1/3}$. When looking at the instances of LCS in different applications three out of the four options frequently appear. In color constancy and intrinsic image computation methods the red channel [2], the green channel i_g [1], as well as the geometric mean [3] have been used. In shadow removal and segmentation the green channel [4] and the geometric mean [5] are popular. In tracking, algorithms using the green channel [6] and geometric mean [7] have

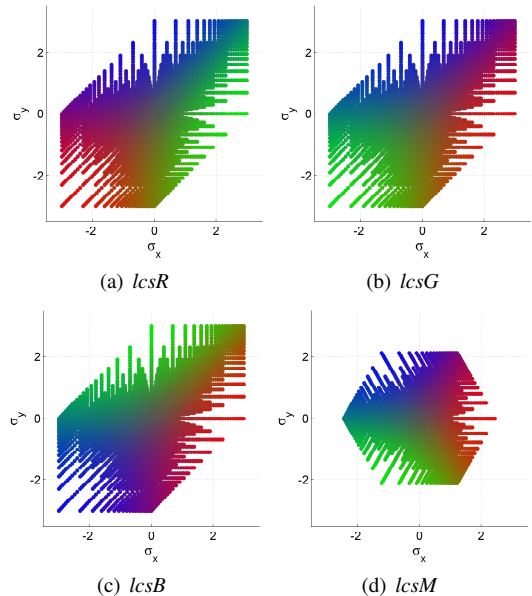


Fig. 1. The projection of an RGB cube to the four LCSs.

been developed. Image stitching preferred the use of the green channel [8]. The geometric mean was employed for object detection [9]. Very recently, the green channel was used for illumination invariant road segmentation [10] and skin color classification [11].

Despite the popularity of LCS there has been so far no systematic evaluation of the impact of the denominator on the color distributions in LCS. We aim to address this issue and provide an analysis of the influence of the normalizing channel. We focus our analysis on classification. Based on metrics describing the clustering of classes in LCS we argue about the influence of the normalizing channel. Evaluations on synthetic and real data demonstrate its impact.

2. THEORY OF LOG-CHROMATICITY SPACE (LCS)

The log-chromaticity space (LCS) is a physics-based color space with excellent illumination-invariant properties [1]. Based on a RGB triplet $\mathbf{i} = (i_r, i_g, i_b)^T$ the respective log-chromaticity value $\sigma = (\sigma_x, \sigma_y)^T$ is computed as follows:

$$\sigma = (\sigma_x, \sigma_y)^T = \left(\ln \left(\frac{i_x}{i_d} \right), \ln \left(\frac{i_y}{i_d} \right) \right)^T, \quad (1)$$

with $x, y, d \in \{r, g, b\}$ and $x \neq y \neq d$. For example, if one uses the green channel i_g as denominator, the LCS values become $\sigma =$

$(\ln(i_r/i_g), \ln(i_b/i_g))^T$. The division of the RGB values by a single channel i_d corresponds to a projection of the RGB data on the plane where $i_d = 1$. Hence, the denominator has a high impact on the clustering of the data in LCS and, therefore, also strongly influences the classification results.

To not favor a color channel one can instead divide by the geometric mean of the three RGB color channels [3]:

$$\rho_c = \ln \left(\frac{i_c}{(\prod_{k \in \{r,g,b\}} i_k)^{1/3}} \right). \quad (2)$$

This transformation results in a projection of the color points on a plane, which contains the point $(0, 0, 0)^T$ and is orthogonal to the vector $(1, 1, 1)^T$. By applying a 2D coordinate system transformation LCS values $\sigma = (\sigma_x, \sigma_y)^T$ are obtained (see [3]). The geometric-mean denominator still preserves the good properties with respect to illumination invariance.

In the remainder of the paper we refer to *lcsR* when the red channel i_r is used (*lcsG* and *lcsB* are similar notations). When the geometric mean is taken as the denominator, we denote it as *lcsM*.

Fig. 1 illustrates the distribution of RGB color values in the four different LCSs. The data was generated by uniformly sampling the RGB cube (see Sec. 4.1). As the division of two intensity channels eliminates brightness variations, two colors having the same chroma and different intensities are projected on the same position in LCS. In all four spaces achromatic colors are transformed to $\sigma = (0, 0)^T$. The color distributions already reveal that the proper selection of the denominator has a high impact on classification. In the next sections we will analyze this effect theoretically and experimentally.

3. CLUSTER ANALYSIS IN LCS

Many different measures have been developed for quantifying the distribution and clustering of data points [12]. For good classification results data points within a class should be similar to each other, while being distinct from data of other classes. We decided to chose the following metrics for *within-class* and *between-class* variance.

For a set $C = \{C_1, C_2, \dots, C_{N_C}\}$ of N_C classes C_i , with $C_i = \{\sigma_1, \sigma_2, \dots, \sigma_{N_i}\}$, we define the *within-class* variance S_w as

$$S_w = \frac{1}{N_C} \sum_{C_i \in C} \frac{1}{N_i} \sum_{\sigma_k \in C_i} (\sigma_k - \mu_i)^T (\sigma_k - \mu_i). \quad (3)$$

The vector $\mu_i = (\mu_{x,i}, \mu_{y,i})^T$ is the mean of the respective class C_i . The number of data points in a class C_i is denoted as N_i .

The *between-class* variance S_b is defined as

$$S_b = \frac{1}{N_C} \sum_{C_i \in C} (\mu_i - \mu)^T (\mu_i - \mu) \quad (4)$$

where $\mu = (\mu_x, \mu_y)^T$ is the mean vector of all the data points. To obtain good classification results the goal is to transform the data to a color space where the *within-class* variance is small and the *between-class* variance is large. Hence, the *between-to-within-ratio* $S = S_b/S_w$ should be as large as possible. We analyze this variance ratio S to derive rules for the proper choice of the normalizing channel i_d for certain classification tasks.

Besides the *between-to-within-ratio* describing the compactness of the data, we also quantify the shape and the spread of an individual cluster. The determinant m_d of the covariance matrix \sum_{lcs} of the LCS values of a cluster,

$$m_d = \det \left(\sum_{lcs} \right) = \lambda_1 \lambda_2, \quad (5)$$

corresponds to the product of the matrix's eigenvalues λ_1 and λ_2 . m_d is proportional to the area of the covariance ellipses and, therefore, covers the spread of a cluster. The eccentricity m_e of a cluster with

$$m_e = \sqrt{1 - \frac{\lambda_2}{\lambda_1}}. \quad (6)$$

denotes how elongated a cluster is. A spherical distribution (i.e. $\lambda_1 = \lambda_2$), would result in $m_e = 0$.

An analysis of S_b and S_w shows the influence of the normalizing channel. The *within-class* variance S_w of Eq. 3 can be transformed to

$$\begin{aligned} S_w &= \frac{1}{N_C} \sum_{C_i \in C} \text{var}(\sigma_{x,i}) + \text{var}(\sigma_{y,i}) \\ &= \frac{1}{N_C} \sum_{C_i \in C} \text{var}(\log(i_x)) + \text{var}(\log(i_y)) + 2\text{var}(\log(i_d)) \\ &\quad - 2\text{cov}(\log(i_x), \log(i_d)) - 2\text{cov}(\log(i_y), \log(i_d)). \end{aligned} \quad (7)$$

The variance of $\log(i_d)$ is weighted twice as much as the other channels. Thus, the RGB channel with the smallest variance of the logarithm should be the normalizing channel. However, the magnitude of S_w also depends on the covariances $\text{cov}(\log(i_x), \log(i_d))$ and $\text{cov}(\log(i_y), \log(i_d))$. If a cluster exhibits a very large covariance between two channels, it might be beneficial to chose the remaining channel as denominator – the large covariance then does not occur in the calculation. A large negative covariance, however, is favorable.

The *between-class* variance S_b in Eq. 4 can be expanded to

$$\begin{aligned} S_b &= \frac{1}{N_C} \sum_{C_i \in C} (\mu_{x,i} - \mu_x)^2 + (\mu_{y,i} - \mu_y)^2 \\ &= \frac{1}{N_C} \sum_{C_i \in C} \mu_{x,i}^2 + \mu_{y,i}^2 + \mu_x^2 + \mu_y^2 - 2\mu_{x,i}\mu_x - 2\mu_{y,i}\mu_y. \end{aligned} \quad (8)$$

A large S_b is obtained when the distance of all class means to the global mean is large. In LCS the magnitude of the absolute mean value of a coordinate, e.g. of $\sigma_x = \log(i_x/i_d)$, is dependent on the logarithm and the ratio: when the ration i_x/i_d is much larger or lower than 1, then the absolute mean value will be large. It is difficult to predict the LCS with the largest S_b in advance.

The analysis of the *between-class* and *within-class* variance does not offer any guidance on the best *between-to-within-ratio*. The *between-class* variance depends mainly on the class-specific and global means in LCS. The *within-class* variance is based on the variance and covariances of the logarithmic RGB values.

4. EXPERIMENTAL ANALYSIS

Experiments on synthetic data further clarify the clustering analysis presented in Sec. 3. The evaluation on real data illustrates how these conclusions generalize to classification problems on real images.

4.1. Synthetic Data

The synthetic data was generated by uniformly sampling the RGB cube with intensities $i_c \in [0, 1]$ and a step size $\tau = 0.1$ (see Fig. 2(a)). To not introduce a bias to the data by handling the division by zero, colors, where at least one channel was zero, were excluded. The set of RGB colors was evenly divided into three clusters (C_r, C_g and C_b) corresponding to the reddish, greenish and bluish colors.

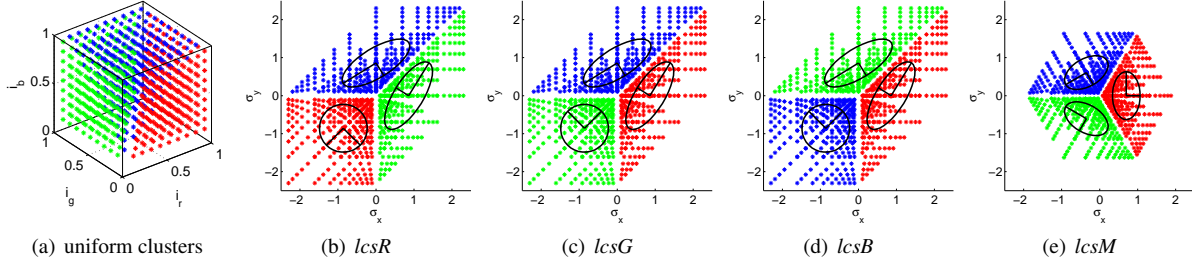


Fig. 2. Results on synthetic data with clusters of equal sizes. The distributions of the three clusters differ, depending on the normalizing channel. The covariance ellipses illustrate the spread of the clusters.

Fig. 2 illustrates the distribution of the three clusters of equal sizes in the four different LCSs. The covariance ellipses, centered at the mean of each cluster, illustrate the spread and the shape of the clusters. It is clearly visible that the single channel denominators introduce a bias to the shape of the distributions. This observation is supported by the eccentricity measure (see Tab. 2), as there, for instance, the reddish cluster C_r only has a circular shape (m_e close to zero) when the red channel i_r is taken as denominator. The remaining two clusters have an elongated shape. This bias, which is introduced in $lcsR$, $lcsG$ and $lcsB$, is not present at $lcsM$. Using the geometric mean as denominator results in three clusters having the same eccentricity m_e . Although the single channel denominators introduce a bias in the shape of the clusters, the spread of the clusters in those spaces is the same (i.e. same m_d across $lcsR$, $lcsG$ and $lcsB$). In the $lcsM$ space the spread is also the same across the different clusters, but compared to the other spaces the spread of the data points is lower and, hence, more compact (i.e. lower m_d). Due to this compactness of $lcsM$, the *between-to-within* ratio S is not affected (see Tab. 1). It is the same for all LCSs. Hence, in uniformly distributed color channels the denominator does not influence *between-to-within* variance but has a strong impact on the shape of the clusters.

We also generated synthetic data where the distributions in the three clusters are not equal. Fig. 3(a) shows an example, where the size of the red cluster C_r is reduced by removing those color points closer to C_g and C_b (i.e. data having a yellowish or magenta chroma). In other sets, the same reduction was done for the both other clusters or two of the three clusters were reduced. The results for the reduced C_r are shown in Tab. 1 and Fig. 3. If the size of the reddish cluster is reduced, the ratio S is higher, when the green or the blue channels are chosen as denominator. The red channel as normalizer results in the lowest S . The clustering performance of $lcsM$ is between the best (i.e. $lcsG$ and $lcsB$) and the worst (i.e. $lcsR$) results. These observations are consistent across all our synthetic data sets.

One can conclude that the $lcsM$ has the advantage of not introducing a bias in the color distributions. Furthermore, the clustering performance of $lcsM$ has always been between the best and the worst results. Hence, for classification we suggest the use of $lcsM$ when one requires a quick solution. However, when prior knowledge on the distributions of color is available, then one of the other LCSs may lead to a better result. Due to the high amount of dependencies in the *between-to-within* ratio it is difficult to predict the best color space by analyzing the means and variances of the RGB channels.

4.2. Real data – Skin Classification

Our analysis of the normalizing channel can lead to a more effective LCS. Consider, for example, the application of skin classification, where based on the respective LCS values a color pixel is classified

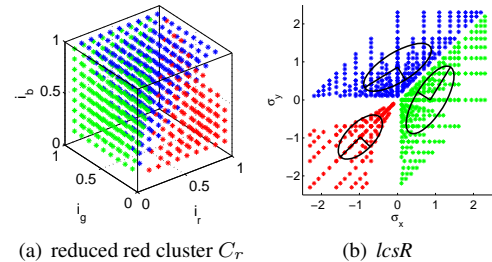


Fig. 3. Results on synthetic data with a reduced reddish cluster C_r . The distributions of the clusters are illustrated for $lcsR$.

| | uniform clusters | | | reduced C_r | | |
|--------|------------------|-------|-------|---------------|-------|-------|
| | S | S_b | S_w | S | S_b | S_w |
| $lcsR$ | 0.93 | 0.98 | 1.05 | 1.20 | 1.22 | 1.01 |
| $lcsG$ | 0.93 | 0.98 | 1.05 | 1.28 | 1.10 | 0.86 |
| $lcsB$ | 0.93 | 0.98 | 1.05 | 1.28 | 1.10 | 0.86 |
| $lcsM$ | 0.93 | 0.49 | 0.53 | 1.25 | 0.57 | 0.46 |

Table 1. Clustering metrics S , S_b and S_w for the uniform clusters and data with reduced red cluster C_r .

as skin ω_s or non-skin ω_n .

As the manner in which a decision is taken varies for different classifiers, the *between-to-within* ratio S as defined in Sec. 3 does not generalize well to all of them. The performance of the different LCSs was evaluated using the false-positive rate (FPR), the true-positive rate (TPR) and, if possible, the ROC curves [13]. We used the Jones and Rehg [14] database (8 960 non-skin and 4 659 skin images). One half of the data was used for training, the other half for testing. The images are arbitrary web images and, hence, are gamma corrected. Although the theory of LCS is provided for linear intensities, the consideration of gamma is beyond the scope of this paper.

Nearest Mean Classification. A color value is classified as ω_s , if it is closer to the trained mean value of the skin cluster than to the mean of the non-skin cluster. The results of the classification are shown in Fig. 3. The $lcsR$ leads to the best skin classification performance, while the worst rates (besides RGB) are achieved by $lcsB$. Using the geometric mean as denominator results in a performance lying between the both.

Probabilistic Approach. To evaluate the classification performance using the different LCSs in combination with a probabilistic approach, we evaluated the method by Jones and Rehg [14]. A LCS

| | $m_e(C_r)$ | $m_e(C_g)$ | $m_e(C_b)$ | $m_d(C_r)$ | $m_d(C_g)$ | $m_d(C_b)$ |
|-------------|------------|------------|------------|------------|------------|------------|
| <i>lcsR</i> | 0.061 | 0.924 | 0.924 | 0.158 | 0.158 | 0.158 |
| <i>lcsG</i> | 0.924 | 0.061 | 0.924 | 0.158 | 0.158 | 0.158 |
| <i>lcsB</i> | 0.924 | 0.924 | 0.061 | 0.158 | 0.158 | 0.158 |
| <i>lcsM</i> | 0.816 | 0.816 | 0.816 | 0.053 | 0.053 | 0.053 |

Table 2. Measures for the shape and spread of the clusters, when the clusters are uniform (see Fig. 2).

| | <i>lcsR</i> | <i>lcsG</i> | <i>lcsB</i> | <i>lcsM</i> | <i>RGB</i> |
|------------|--------------|-------------|-------------|-------------|------------|
| <i>TPR</i> | 0.766 | 0.762 | 0.730 | 0.754 | 0.730 |
| <i>FPR</i> | 0.229 | 0.230 | 0.238 | 0.231 | 0.358 |

Table 3. Results of skin detection using nearest mean classification.

color σ is assigned to the skin class ω_s , if

$$P(\sigma | \omega_s) / P(\sigma | \omega_n) \leq \theta. \quad (9)$$

If the ratio of the conditional probabilities is lower than a threshold θ , the color is assigned to the non-skin class ω_n . To apply the method, color histograms are required. For the LCSs we used $\sigma_{\{x,y\}} \in [-5, 5]$ with 1000 bins in each dimension. For RGB 32 bins were used, as recommended in [14].

The ROC curves in Fig. 4 reveal the significant impact of the normalizing channel on the classification performance. Using the blue channel i_b as denominator results in a recognition performance 25.9% better compared to the red channel (worst recognition performance) for a false-positive rate of 10%. The green channel, a popular choice as normalizing channel, results in an intermediate curve. The geometric mean performs slightly worse than *lcsB*. Nevertheless, for a false-positive rate of 10%, the true-positive rate of *lcsB* is about 2.9% better than *lcsM*.

Comparing the results of the nearest mean classifier with the probabilistic approach, the ranking of the four LCSs differs. The *LcsB*, for instance, results depending on the approach in the best and worst recognition performance. In our experiments, the geometric mean always achieved good results, however, always was outperformed by another single-intensity denominator.

5. CONCLUSIONS

We provide an analysis of the impact of the normalizing channel on the color distributions in LCS. The *lcsM* has the advantage of not introducing a bias in the color distributions. In our evaluation on synthetic data its clustering performance has always been between the best and the worst results. For skin classification the *lcsM* led to good results, but was always outperformed by another single-intensity denominator. Hence, for classification we suggest the use of *lcsM* when one requires a quick solution. However, the use of one of the three other normalizing channels may lead to a better result. Compared to the most popular LCSs, i.e. *lcsM* and *lcsG*, we could improve the skin classification performance by about 2.9% and 12.9%, respectively, by taking the blue channel as denominator.

6. ACKNOWLEDGMENT

The authors gratefully acknowledge funding of the Erlangen Graduate School in Advanced Optical Technologies (SAOT) by the German National Science Foundation (DFG) in the framework of the excellence initiative. Eva Eibenberger is supported by the International Max Planck Research School for the Physics of Light (IMPRS-PL).

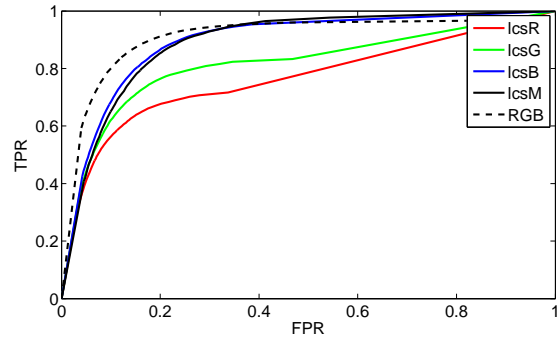


Fig. 4. ROC curves of the four different LCSs using the probabilistic approach.

7. REFERENCES

- [1] G. D. Finlayson and S. D. Hordley, “Color Constancy at a Pixel,” *J. Opt. Soc. Am. A*, vol. 18, no. 2, pp. 253–264, 2001.
- [2] Q. He and C.-H. H. Chu, “Intrinsic Images by Fisher Linear Discriminant,” in *International Symposium Advances in Visual Computing (ISVC)*, 2007, pp. 349–356.
- [3] G. D. Finlayson, M. S. Drew, and C. Lu, “Intrinsic Images by Entropy Minimization,” in *ECCV*, 2004, pp. 582–595.
- [4] C. Lu and M. S. Drew, “Shadow Segmentation and Shadow-Free Chromaticity via Markov Random Fields,” in *Color Imaging Conference*, 2005, pp. 125–129.
- [5] G. D. Finlayson, M. S. Drew, and C. Lu, “Entropy Minimization for Shadow Removal,” *Int. J. Comput. Vision*, vol. 85, no. 1, pp. 35–57, 2009.
- [6] H. Jiang and M. S. Drew, “Shadow Resistant Tracking using Inertia Constraints,” *Pattern Recognit.*, vol. 40, no. 7, pp. 1929–1945, July 2007.
- [7] J. Scandaliaris and A. Sanfeliu, “Discriminant and Invariant Color Model for Tracking under Abrupt Illumination Changes,” in *ICPR*, 2010, pp. 1840–1843.
- [8] O.-S. Kwon and Y.-H. Ha, “Panoramic Video using Scale-Invariant Feature Transform with Embedded Color-Invariant Values,” *IEEE Trans. Consum. Electron.*, vol. 56, no. 2, pp. 792–798, 2010.
- [9] J. Scandaliaris, M. Villamizar, and A. Sanfeliu, “Comparative Analysis for Detecting Objects Under Cast Shadows in Video Images,” in *ICPR*, 2010, pp. 4577–4580.
- [10] J. M. Álvarez and A. M. López, “Road Detection Based on Illuminant Invariance,” *IEEE Trans. Intell. Transp. Syst.*, vol. 11, no. 99, pp. 1–10, 2010.
- [11] B. Khanal and D. Sidibé, “Efficient Skin Detection under Severe Illumination Changes and Shadows,” in *International Conference on Intelligent Robotics and Applications (ICIRA)*, 2011, pp. 609–618.
- [12] S. Theodoridis and K. Koutroumbas, *Pattern Recognition*, Academic Press, Inc., Orlando, FL, USA, 4th edition, 2009.
- [13] T. Fawcett, “An introduction to ROC analysis,” *Pattern Recognit. Lett.*, vol. 27, no. 8, pp. 861–874, 2006.
- [14] M. J. Jones and J. M. Rehg, “Statistical Color Models with Application to Skin Detection,” *Int. J. Comput. Vision*, vol. 46, no. 1, pp. 81–96, 2002.